ISTANBUL TECHNICAL UNIVERSITY ★ GRADUATE SCHOOL OF SCIENCE ENGINEERING AND TECHNOLOGY

SINGLE-MOLECULE FORCE EXPERIMENTS OF MOTOR PROTEINS VIA MOLECULAR DYNAMICS SIMULATIONS

M.Sc. THESIS

Mohammad Amin SALEHI TABRIZI

Department of Mechanical Engineering

Thermo-Fluid Program

September 2019

ISTANBUL TECHNICAL UNIVERSITY ★ GRADUATE SCHOOL OF SCIENCE ENGINEERING AND TECHNOLOGY

SINGLE-MOLECULE FORCE EXPERIMENTS OF MOTOR PROTEINS VIA MOLECULAR DYNAMICS SIMULATIONS

M.Sc. THESIS

Mohammad Amin SALEHI TABRIZI
(503151118)

Department of Mechanical Engineering

Thermo-Fluid Program

Thesis Advisor: Assist. Prof. Dr. Mert GÜR

September 2019

ISTANBUL TEKNİK ÜNİVERSİTESİ ★ FEN BİLİMLERİ ENSTİTÜSÜ

MOTOR PROTEİNLERİNİN BİLGİSAYAR ORTAMINDAKİ ÇEKME DENEYLERİNİN MOLEKÜLER DİNAMİK SİMÜLASYONLARIYLA GERÇEKLEŞTİRİLMESİ

YÜKSEK LISANS TEZİ

Mohammad Amin SALEHI TABRIZI
(503151118)

Makina Mühendisliği Anabilim Dalı

Isı-Akışkan Programı

Tez Danışmanı: Dr. Öğr. Üye. Mert GÜR

Eylül 2019

Mohammad Amin Salehi Tabrizi, a M.Sc. student of ITU Institute of Science and Technology 503151118, successfully defended the thesis entitled "SINGLE-MOLECULE FORCE EXPERIMENTS OF MOTOR PROTEINS VIA MOLECULAR DYNAMICS SIMULATIONS", which he prepared after fulfilling the requirements specified in the associated legislations, before the jury whose signatures are below.

Thesis Advisor: **Assist. Prof. Dr. Mert GÜR** .....
Istanbul Technical University

Jury Members: **Assoc. Prof. Dr. Gizem DİNLER DOĞANAY**.....
Istanbul Technical University

Prof. Dr. Serdar DURDAĞI .....
Bahçeşehir Üniversitesi

Date of Submission : 03 May 2019
Date of Defense : 02 September 2019

To my dear family

FOREWORD

I would like to express my appreciation and thanks to my advisor, Assist. Prof. Mert Gur. I would like to thank you for encouraging my research and for allowing me to grow as a research scientist. Your advice on both research as well as on my career have been invaluable. I also want to thank you for making my defense an enjoyable moment, and for your brilliant comments and suggestions.

Special thanks to my family. Words cannot express how grateful I am to my mother and father for all of the sacrifices that they have made on my behalf. Their prayer for me was what sustained me thus far. I would also like to thank all of my friends who incented me to strive towards my goal. I am very grateful for everything they have done for me.

My heartful thanks to my dear friends and colleagues Mert Gölcük, Sema Zeynep Yılmaz, Elhan Taka, Ceren Kılınç, and Onur Özer for their help and joyful memories we shared.

In addition, I gratefully acknowledge the support of TÜBITAK grant no. 215Z398.

September 2019

Mohammad Amin SALEHI TABRIZI

TABLE OF CONTENTS

Page

ABBREVIATIONS

ATP : Adenosine Triphosphate

ADP : Adenosine Diphosphate

RNA : Ribonucleic Acid

DNA : Deoxyribonucleic Acid

mRNA : Messenger RNA

MTBD : Microtubule-Binding Domain

PT : Proximal Tail

CaM : Calmodulin

MD : Molecular Dynamics

NMR : Nuclear Magnetic Resonance

QM : Quantum Mechanics

MM : Molecular Mechanics

SAH : Single Alpha Helix

AMBER : Assisted Model Building with Energy Refinement

CHARMM : Chemistry at Harvard Macromolecular Mechanics

NAMD : Nanoscale Molecular Dynamics

VMD : Visual Molecular Dynamics

PDB : Protein Data Bank

PSF : Protein Structure File

NVT : Number, Volume, Temperature

NPT : Number, Pressure, Temperature

NVE : Number, Volume, Energy

RMSD : Root Mean Square Deviation

SASA : Solvent Accessible Surface Area

LIST OF FIGURES

Page

SINGLE-MOLECULE FORCE EXPERIMENTS OF MOTOR PROTEINS VIA MOLECULAR DYNAMICS SIMULATIONS

SUMMARY

Due to their significant role in muscle contraction and intracellular cargo transport, motor proteins have gained much interest in recent years. Motor proteins convert the energy obtained by ATP hydrolysis into mechanical energy. Molecular Dynamics (MD) simulations is a powerful methodology to investigate the mechanic properties of motor proteins. In this thesis work, MD simulations of myosin and dynein were performed. All myosins have a conserved domain organization: an N-terminal motor domain, a neck region (lever arm) containing one to six IQ motifs that provide binding to light chains or calmodulin, and a highly variable tail domain. Large-scale stepping of myosin VI is facilitated by the extension of the proximal tail domain of lever arm region of myosin. Proximal tail domain of lever arm region of myosin was extended by steered molecular dynamics (SMD) simulations. In SMD simulations the center of mass of a group of atoms is pulled along a vector. MD simulations results of proximal tail domain of lever arm region were compared with literature and our results were validated. As a second step, the linker structural transition of the motor protein dynein between its pre-Powerstroke and post power stroke states were modeled using SMD simulations. Cytoplasmic dynein is a homodimer and consists of two identical heavy chains. The heavy chain includes a motor domain that comprises a ring of six AAA+ domains (AAA1-6) and four structures protrude: stalk, linker, buttress, and C-terminal domains. In the dynein pre Powerstroke state the linker is in a bent conformation while in the post power stroke state it is in a straight conformation. A similar procedure as it was applied to myosin was performed for dynein and the transition was partially modeled. The SMD simulations performed at finite constant velocities provided us irreversible work values for this transition at the selected velocities.

MOTOR PROTEİNLERİNİN BİLGİSAYAR ORTAMINDAKİ ÇEKME DENEYLERİNİN MOLEKÜLER DİNAMİK SİMÜLASYONLARIYLA GERÇEKLEŞTİRİLMESİ

ÖZET

Kimyasal enerjiyi mekanik işe dönüştürebilen biyolojik moleküller motor proteinleri veya moleküler motorlar olarak bilinir. Bu nanometre büyüklüğündeki makineler, genetik bilgi aktarımı, hücre içi taşıma, organizasyon ve işleyişi gibi temel hücresel süreçlerinde önemli görevler alırlar. İnsan vücudunda birçok farklı tip moleküler motor vardır. Miyozin motor proteinleri kas kasılmalarında rol oynamaktadırlar. Diğer bir motor proteini sınıfı olan dineinler, hücre içerisinde mikrotübüller üzerinde eksi yönde taşımayı gerçekleştirmekle görevlidirler. Kinezin motor proteinleri de miktrotübüller üzerinde iki yönde de taşımayı sağlarlar. Tüm bu nano ölçekli makineler kimyasal enerjiyi benzer prensipler kullanarak mekanik işlere dönüştürürler. Bu katalitik işlemler sırasında salınan kimyasal enerjinin bir kısmı bir şekilde moleküler motorlar tarafından mekanik harekete yönlendirilir. Son yıllarda motor proteinleri, moleküler motor dinamiğinin temel prensiplerini ve mekanizmalarını ortaya çıkarmayı amaçlayan yoğun araştırma çabalarına konu olmuştur. Motor proteinlerinin mekanik özelliklerinin incelenmesi için Moleküler Dinamik (MD) simülasyonları önemli bir yöntemdir. Bu tez çalışmasında, MD simülasyonları kullanılarak miyozin ve dinein motor proteinlerinin MD simülasyonları yapılmıştır. Çalışmanın ilk adımında literatürde yapılan bir çalışma ve uygulanan teknik tekrar edilerek uygulanan yöntemin uygulayış şekli ve elde ettiğimiz verilerin doğruluğu valide edilmiştir. Söz konusu validasyon sonrasında ise, tezin ikinci aşaması olarak ilk aşamada uygulanan yöntem önceden MD simülasyonları ile çalışılmamış bir protein hareketini modelleme amacıyla uygulanmıştır

Çalışmanın ilk aşamasında miyozin VI proteinin MD simülasyonları gerçekleştirilmiştir. Motor proteinlerinden birisi olan miyozin VI'nın büyük ölçekli adımlar atabilmesi kuvvet kolu bölgesinin proksimal kuyruk (PT) bölgesinin uzayabilmesi/genişleyebilmesi sayesinde gerçekleşmektedir. Bu tez çalışmasında yönlendirilmiş MD simülasyonları gerçekleştirerek PT bölgesinin üç alfa sarmalı uzatılıp PT bölgesi genişletilmiştir.

MD simülasyonlarında kullanılacak olan miyozinin VI kolunun yapısı, Protein Veri Bankasından (PDB) elde edilmiştir. Miyozinin büyük ve asimetrik bir yapısı bulunmaktadır. Uzun bir proksimal kuyruğu (PT) ve iki adet küre şeklinde kafa bölgesi bulunmaktadır. Pt bölgesinin uzama/genişleme hareketinde önemli bir görevi olan IQ-kalmodulin motifi ve PT bölgesinin bu simetrik yapının bir tarafında bulunmakta ve diğer kısımlardan ayrılmaktadır. IQ-kalmodulin motifi kuvvet kolu hareketini düzenleyen önemli sekans bölgesi içermekte iken, PT bölgesi miyozin proteininin mikrotübüle bağlanmasını sağlayan genişleyen kısım olarak görev yapmaktadır. Yapının incelenmesinde önemli olan ilk adım olarak gerçekçi bir hücre ortamının oluşturulabilmesi için, IQ-kalmodulin-PT yapısı belirli boyutlardaki bir su kutusuna yerleştirildi ve 50 mM potasyum klorür (KCl) ile nötralize edildi. Bu işlem sonrasında,

oluşturulan sistemin kararlı durumuna ulaşabilmesi için, oluşturulan sistem dengeye getirildi. Bu adım, birinci seviyesinde yapının tüm omurgasına baskılamalar uygulanarak ve ikinci seviyede kısıtlamalar uygulanarak 5 seviyede gerçekleştirildi. Üçüncü adım olarak, PT bölgesinin ilk rezidüsü sabitlenerek ve son rezidüsüne ise sabit hız çekme kuvvetinin uygulanarak SMD simülasyonları gerçekleştirildi. Bulunan veriler literatür ile karşılaştırılarak uygulanan yöntem valide edilmiştir.

Tez çalışmanın ikinci aşamasında, başka bir motor proteini olan dineinin güç stroku öncesi ve güç stroku sonrası kuvvet kolunun yapısındaki değişim modellenmiştir. Sitoplazmik dinein, birbirine bağlanmış iki aynı mikro moleküler makineden oluşan ve her biri kimyasal enerjiyi işe dönüştüren bir hekzamerik halka şekilli katalitik alan içeren homodimerik bir motordur. Her bir dinein monomerinde hekzamerik halka 6 adet AAA+ bölgesinden oluşmaktadır ve bu bölgeye motor bölgesi veya baş bölgesi denmektedir. Bu katalitik halkadan çıkan 4 uzantı vardır: sap, payanda, kuvvet kolu ve C-terminal bölgesi. Dineinin kuvvet kolu ATP hidrolizinden gelen enerjiyi kullanır ve güç strokları arasındaki geçişte bükülme ve açılma haraketi yapar. Güç stroku öncesinde kuvvet kolu bükük halde iken güç stroku sonrası düz halde bulunmaktadır. Dinein proteinin güç stroku sonrası halden güç stroku öncesi hale geçişine hazırlama stroku denilmektedir. Miyozin için uygulanan benzer adımlar izlenerek, dinein motor proteininin güç stroku öncesi ve güç stroku sonrası arasındaki hazırlama stroku sırasında gerçekleştirdiği kuvvet kolu hareketleri kısmı olarak modellenmiş ve bu çekme hızlarında uygulanan tersinmez iş miktarı ölçülmüştür.

Miyozin uzantısına benzer şekilde, SMD işlemi kuvvet ve gevşetme uygulanarak gerçekleştirilmiştir. Önceki çalışmadan farklı olarak, SMD simülasyonu sırasında protein omurgasındaki rezidüler sabitlenmek yerine sınırlandırılmıştır. Dineinin bağlayıcı alanındaki üç alfa helis seçilmektedir ve her alfa sarmalında, SMD simülasyonu sırasında bir bozulmaya neden olmayacak bir mesafeden bir artık belirlenmektedir. PDB' den elde edilen ilk yapı, insana ait dineininin ön güç stroku durumunu belirten dinein-2 motor proteinine aittir. Bu yapı literatürde[1] MD simülasyonları ile modellenmiştir. Sunulan tez çalışmasında literatürdeki MD simülasyonundan elde edilen suda çözünmüş dinein protein yapısı[1] kullanılmıştır. Güç stroku öncesi, kuvvet kolu alanı bükülmüş vaziyettedir (PDB: 4RH7). İkinci yapıda ise, kesilmiş mikrotübül bağlanma bölgesi olan dinein motor MTBD'nin bir parçasına sahip değildir ve adenozin difosfat (ADP) buna bağlanmıştır. Bu dinein, A monomerinde antiparalel sarmallı düz bir sapa ve daha kısa sarmallı sarmaldan yapılmış kıvrılmış sapa sahiptir (PDB: 3VKG). 4RH7 ve 3VKG dinein yapılarının istenen parçaları birbirine hizalanmıştır. 4RH7 dineininin bağlayıcı alanındaki üç alfa helis seçildi ve her alfa sarmalında, SMD simülasyonu sırasında bir bozulmaya neden olmayacak bir mesafeden bir artık tespit edimiştir. Seçilen amino asitlerin (1264, 1309, 1325) alfa karbonlarının kütle merkezi ölçülmüştür. 3VKG yapının birleştiricisi için 3 alfa helis de seçilir ve uygun mesafelerdeki kalıntılar belirledi. Seçilen amino asitlerin alfa karbonlarının kütle merkezi (1531, 1572, 1588) ölçmüştür. Bu kütle merkezi arasında bir vektör oluşturulmuştur. Dinein kuvvet kolunun hareketinin modellenmesi için by vektör boyunca söz konusu atomlara çekme kuvveti uygulanmıştır. Bu SMD simülasyonlarında, bağlayıcının menteşe bölgesi olan 1415 ila 1425 arasındaki artıkların alfa karbonları sabit olarak alındı. SMD simülasyonlarında yay sabiti olarak 25 kcal / mol Å2 ve çekme hızı ise 1 Å / ns olarak seçildi. Her SMD simülasyonu 5ns ucunluğunda olup toplamda 5 tane SMD simülasyonu gerçekleştirilmiştir. SMD simülasyonları arasında 10ns uzunluğunda yapısal kısıtlayıcı simülasyonlar gerçekleştirilmiştir. Bu simülasyonlarda kısıtlayıcı potansiyellerin uygulanacağı

atomlar 1415, 1425, 1264, 1309, ve 1325 amino asitlerin alfa karbon atomları seçilmiştir. Yay sabiti kısıtlama simülasyonlarında 5 kcal / mol $Å^2$ olarak seçildi. Toplamda 5 SMD ve 4 sınırlandırma simülasyonu gerçekleştirilmiştir. Bu simülasyonların sonucunda kuvvet kolu güç stroku öncesi yapısına yaklaşmıştır.

1. INTRODUCTION

1.1 Proteins

Proteins are macromolecules which are highly important for human body functions. Proteins are polypeptides made by 20 types of amino acids and these amino acids determine the structure of the protein by varying sequences [2]. There are a lot of proteins in the cells of various structures. Proteins can have various essential roles for cells such as acting as catalysts accelerating biological processes, storing vital molecules such as oxygen, providing mechanical support and transport inside the cell [3]. Motor proteins are a family of proteins that are responsible for various processes such as providing muscle contraction and transporting vesicles and biological loads in the cytoplasm. Motor proteins are powered by ATP hydrolysis and, they are able to move along actin filaments and microtubules. Motor proteins consist of myosin, kinesin and dynein superfamilies. In this thesis, a member of each of the myosin and dynein superfamilies were used in the simulations.

1.1.1 Myosin proteins

Myosin superfamily of motor proteins power muscle contraction and move along actin filaments [4, 5]. Actin filaments are like tracks that have two ends, which are a negative end and a positive end. Generally, the positive pointed end of filaments is directed to membrane of cell and inversely, minus pointed end is directed to inside cell [6]. Myosin proteins move along this actin filaments by converting energy from ATP hydrolysis to mechanical work. All myosins have a conserved domain organization: an N-terminal motor domain, a neck region (lever arm) containing one to six IQ motifs that provide binding to light chains or calmodulin, and a highly variable tail domain (Roberts 2004). The catalytic cycle of actin-myosin starts with ATP hydrolysis in the motor domain of myosin occurring in the absence of actin. As a result of the ATP hydrolysis, release of Pi and MgADP [4, 7] induces conformational change in the motor domain of myosin [8-10]. The conformational change in the motor domain provides movement, known as the Powerstroke, of the lever arm of the myosin. The

magnitude of the Powerstroke, or step size of myosin, is determined by the length of its lever arm.

Myosin VI is a unique member of the myosin family that walks towards the minus end of the filament, unlike other myosins that walk towards the plus end. Myosin VI is responsible for various functions inside the cell such as transporting vesicles during endocytosis [11], maintenance of function and structure of Golgi [12], and hair cell mechanics in hearing [13]. Myosin VI includes: an ATP binding site and a unique insert-2 domain associating with calmodulin (CaM) at its actin-binding motor domain; an IQ motif; a proximal tail (PT) domain that forms a three-helix bundle [14]; an a-helical medial tail (MT) domain; a distal tail (DT) domain; and a cargo binding domain (CBD) [15]. Despite having short lever arms, myosin VI can walk with large step size about 30-36 nm and this function cause doubt about swinging lever arm hypothesis, which claims that the length of the lever arm specifies the step size of a motor protein. The proximal tail (PT) domain of myosin can extend to triple its length, thus provides the extension of the lever-arm long enough to accommodate a large step size of 30–36 nm [16].

1.1.2 Dynein motor proteins

Dynein superfamily of motor proteins provides transport of different cargos such as membrane-bound organelles, protein complexes, RNAs and viruses inside the cell [17]. Dyneins move towards the minus end of microtubules by using energy from ATP-hydrolysis [18]. Cytoplasmic dynein is a homodimer and consists of two identical heavy chains. The heavy chain includes a motor domain that comprises a ring of six AAA+ domains (AAA1-6) and four structures protrude: stalk, linker, buttress, and C-terminal domains [19-21]. Each AAA+ domain has a large (AAAL) and small (AAAS) subunits. Only four AAA sites (AAA1-4) have ability to bind ATP and AAA1 is the most significant site which is essential for mobility [22, 23]. AAA5 and AAA6 do not have the ability to bind ATP and these sites provide structural support for the stalk and buttress. In the absence of nucleotides in the AAA1 site, dynein linker takes a straight conformation. ATP binding and hydrolysis induce linker to take a bent conformation [23, 24]. The stalk of dynein has a microtubule-binding domain (MTBD) at its end. The tail of dynein provides dimerization and cargo binding [21, 25, 26].

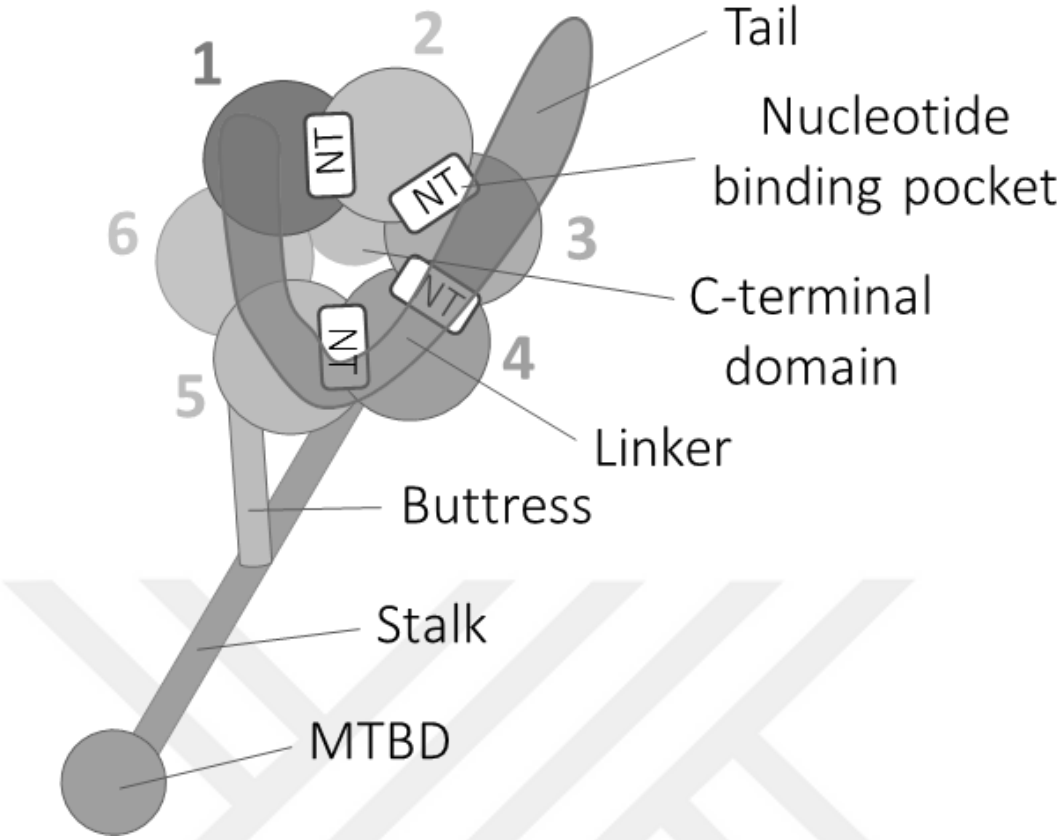

Figure 1.1: Structure of dynein.

In the mechanochemical cycle of dynein, firstly AAA1 site of dynein is empty (apo) and the linker is in straight conformation called post-powerstroke state [27]. In this state, dynein is attached to the microtubule. ATP binding to AAA1 causes linker to undergo conformational change and take a bent conformation called pre-powerstroke. After ATP binding, dynein loses connection with the microtubule [23]. ATP bound to AAA1 is hydrolyzed into ADP and Pi, results in rebinding of dynein to the microtubule. Pi is released from AAA1, this provides linker to turn back to its straight conformation. Dynein returns to its initial state of the cycle after ADP is released.

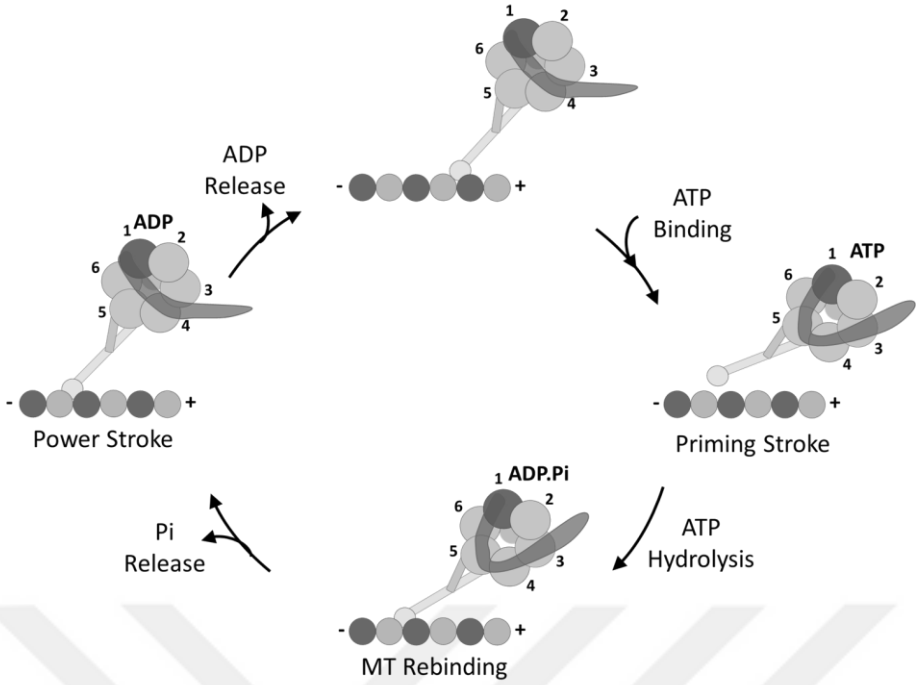

Figure 1.2: The motility process of dynein motor protein.

1.2 Purpose of the Thesis

The purpose of the thesis is to perform in silica single-molecule experiments and model structural transitions in motor proteins myosin and dynein. As the first case, lever arm extension of myosin VI is performed to benchmark and validate our results with simulation data in the literature. After validation, a similar methodology is applied to explore the linker movement of dynein. By doing so, the conformations sampled during linker transitions and the reversible work required to move the linker at finite speed are obtained. These simulation results will contribute to the understanding of the functional mechanisms of these motor proteins.

1.3 Literature Review

In the study by Sweeney and Houdusse [28], it is explained that the different domains in myosin VI structure have particular roles in its function. Lever arm region encompasses various number of IQ motifs in a helix structure that provides calmodulin binding. Insertion segment between the converter and lever arm, so-called reverse gear accomplishes reverse directionality in myosin VI movements on actin filaments through supplying minimum length of the lever arm. Besides these functions of particular structures in myosin VI, most of the articles investigate the other unique

property of myosin VI which is its dimerization. In the studies of Spink et al. [29] and Phichith et al. [30]., it is suggested that cargo binding induces myosin VI to dimerize. Spink et al. [29] performed X-ray scattering experiments and considering the resulted data, they concluded that in the absence of cargo binding process, full-length myosin VI exists as a monomer. In this condition, some intramolecular interactions are leading to block dimerization by cargo-binding domain. In the study of Phichtich et al. (2009), it is shown that binding optineurin, which is a dimeric cargo adaptor protein, induces myosin VI to dimerize internally. This binding omited the inhibition of cargo binding domain and permits the affinity between two unfolded monomers of cargo domains to start dimerization [30]. Spink et al. [29] also described the myosin VI structure and proposes that the primary reason for the 36 nm large steps of myosin is extension of single alpha helix. In their study, it is shown that conformation of SAH is classic a-helical and it is sufficient to fulfill functional lever arm extension with the help of folded three-helix bundle. It means that SAH is dominating component in extension. In opposition, Mukhejra et al.[14] states that the lever arm extension is caused by unfolding of three-helix bundle, known as proximal tail, only after the dimerization. It illustrates that in this view, single alpha helix segment is just a spacer among motor and cargo. This means that single alpha helix does not take part in lever arm extension process.

Espinoza-Fonseca et al. [31] performed Molecular Dynamics (MD) simulations of the light chain of smooth muscle myosin to understand the structural basis of myosin. Their simulations provide insights into the details of the myosin structure which are not revealed by experiments. Liu et al. [16] performed MD simulation studies upon the lever arm extension process with considering the Mukhejra et al.[14] achievement and investigated the details of three bundle extension. In this MD study, it is demonstrated that calmodulin has significant effect on facilitating extension path and it contributes to stabilization of lever arm after extension [16]. Mugnai et al.[32] provide the molecular basis for Powerstroke of myosin VI motility by using a coarse-grained model. They demonstrated that the powerstroke occurs in two steps. Also by analyzing the trajectories they discovered that rotation is mostly uncoupled from the motor domain.

The other interesting family of motor proteins that carry cargo and move towards the end side of microtubules is dynein. There are a few MD studies of dynein in the

literature. Choi et al. [33], performed protein-protein docking simulations of dynein structure with low MT binding affinity. By doing so they obtained a model for high MT affinity dynein structure. They performed simulations with wild type and mutant dynein for docking. Redwine et al. [34], modelled the pseudo atomic models of low and high MT binding affinity dynein by combining cryo-electron microscopy and MD simulations. Nishikawa et al. [35], obtained the crystal structure of *Mus musculus* dynein stalk (PDB ID: 3WUQ) and performed MD simulations for comparing this structures with available structures in literature. Kamiya et al. [36], performed MD simulations for two dynein models (ADP and ATP bound) and observed the structural changes. In a very recent study [37], MD simulations of the human dynein in its pre-power stroke state (PDB ID: 4RH7 [27]) and its engineered constructs were performed. They changed the length and angle of the stalk, and observed that the direction of the linker swing vector was altered into the reverse direction along the MT.

2. MATERIAL AND METHODS

2.1 Molecular Dynamics Simulation

Macromolcular structure has The primary thought of molecular dynamics is depend on van der waals and Boltzmann but new period of it started with the research on hard-sphere liquids in the late 1950s. Next step in the evolution of molecular dynamic was done by Rahman, [38] on a molecular dynamics simulation of liquid argon in 1964. After 25 years since the first molecular dynamics simulation, the biological macromolecule which is called bovine pancreatic trypsin inhibitor in 1977 by McCammon et al [38] . During the decates, through efforts of the researchers such as verlet, Anderson, Nose and parrinello, soo much improvement and development were occured within the aspect of atomic modelling and molecular dynamics simulation and due to it, we can use this method in different scientific areas.

One of the advantages of molecular dynamics simulation which has a great role in the increasing applications of it, is that final details contributed to every particle motions as a function of time, can be obtained. These information is so useful to understand the specifications of system in a easy way with comparing of experiments. Other significant previlige of simulations, is that for investigating the special property of system, it is possible to control parameters which is involving in the simulation by the user [39].

In the MD simulations atoms move according to the Newtonian equations of motion [40];

$$m_\alpha \overrightarrow{r_\alpha} = -\frac{\partial}{\partial \overrightarrow{r_\alpha}} U_{total}(\overrightarrow{r_1}, \overrightarrow{r_2}, \dots, \overrightarrow{r_N}), \qquad \alpha = 1,2, \dots, N \tag{1}$$

where the mass of atom α as refers m_α, position of atom refers as $\overrightarrow{r_\alpha}$, and the total potential energy refers as U_{total}. Total potential energy depends on all atomic positions and coupling with motion of atoms.

In the MD simulations, force fields are the crucial part[40]. Because, force fields represent the interaction of atoms in form of simple mathematical equation [41].

$$U = \sum_{bonds}\frac{1}{2}k_b(r-r_0)^2 + \sum_{angles}\frac{1}{2}k_\alpha(\theta-\theta_0)^2 + \sum_{torsions}\frac{V_n}{2}[1+\cos(n\phi-\delta)] + \sum_{improper}V_{imp} + \sum_{LJ}4\epsilon_{ij}\left(\frac{\sigma_{ij}^{12}}{r_{ij}^{12}} - \frac{\sigma_{ij}^{6}}{r_{ij}^{6}}\right) + \sum_{elec}\frac{q_i q_j}{r_{ij}} \quad (2)$$

Here the first four terms are the intramolecular and local contributions to the total energy and the remaining terms represent the Lennard-Jones potential and the Coulombic interactions [41].

Moreover, MD simulations use periodic boundary conditions to avoid surface effects [40]. Particles of the system enclosed in a cell. Periodic translations provide infinite number of the cell. One of the particles of the system leaves the cell on one side, simultaneously another particle enters the cell on the opposite side [40].

Another important point of the MD simulation calculations is full electrostatic computations that solves and compute the long-range electrostatic interactions [40]. The Ewald summation is a description of long-distance electrostatic interactions for a periodically bounded, spatially limited system [40].

Simulated systems are accepted as a thermodynamic system [42]. This thermodynamic system has volume (V), number of particles (N), pressure (P), and the total energy (E) properties. According to these properties, MD simulations were done with different ensembles [42].

NVT ensemble: In this ensemble, three thermodynamic parameters involving N, V and temperature (T) are fixed [42]. However, in the laboratory conditions experiments applied under constant pressure [43]. For mimicking the experimental conditions, NPT ensemble is used [43].

2.2 Steered Molecular Dynamics Simulations

SMD is one of the MD sampling method. SMD provides investigation of some of the biological processes, such as ligand unbinding and conformational changes of the biological molecules, on accessible time scales with MD [44]. SMD simulations mimic Atomic-Force Microscopy assays in principle [45].

SMD is a simulation method which an external time-dependent forces are applied to one or more atoms. These are refferred to as SMD atoms. The applications of it, yield significant insight into biological processes such as unbinding of ligand from protein,

moving peptides and unfolding of proteins. In this thesis, constant velocity pulling SMD simulations were performed. In constant velocity SMD simulations the center of mass of the SMD atoms is attached to a dummy atom by a virtual spring [40, 46]. This dummy atom or center is moved at constant velocity and then the force between both is measured via using [40]:

$$\vec{F} = -\nabla U \tag{3}$$

where

$$U = \frac{1}{2} k[vt - (\vec{r} - \overrightarrow{r_0}).\vec{n}]^2 \tag{4}$$

Here U is the potential energy, k is the spring constant, v is pulling velocity, t is the time, $\vec{r}$ is the actual position of the SMD atom or center and $\overrightarrow{r_0}$ is the dummy atom coordinate, and $\vec{n}$ refers the direction of pulling [40].

2.3 System Preparation Of Lever Arm Of Myosin VI

This study based on the Liu et al.[16] study that investigation of lever arm three-helix bundle extension process of myosin VI with SMD simulations and key role of calmodulin. At the first step, lever arm of myosin VI crystal structure (PDB 3GN4 [14]) was obtained.

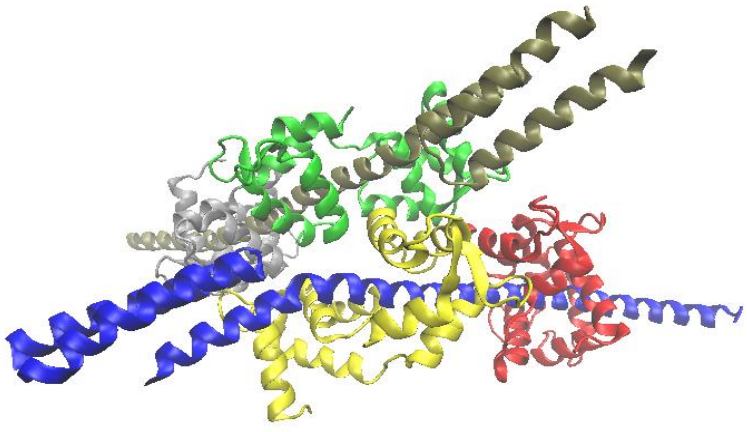

Figure 2.1: Structure of myosin VI lever arm.

On the lever arm of the myosin VI structure a missing region is found between 850 and 863 residues. This missing structure was modelled as loop as proposed in the study

by Liu et al. [14]. As was done by Liu et al. [14]structure was cropped so that the prepared system contained IQ motif (residues 811-833), PT domain (residues 834-913), and apo calmodulin structure that bound the IQ motif.

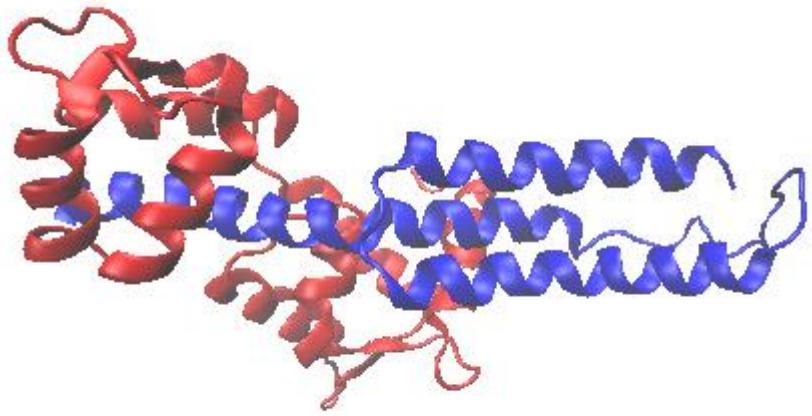

Figure 2.2: Proximal tail domain included three alpha helix (blue) and IQmotif/calmodulin (red).

Hydrogen atoms of the system were added by using "AutoPSF v1.8 " plugin of the VMD software [47]. Then, system was solvated with 24,600 TIP3P explicit water by using "Solvate v1.5" plugin of VMD. The solvated system size was 165 Å × 65 Å × 73 Å. Then, 50 mM KCl were added to system and total system charge was neutralized with KCl by using "Autoionize v1.5" plugin. And, total system size was 73,349 atoms. A cutoff distance for van der Waals (vdW) interactions was set to 12 Å with switching function that started at 10 Å and reach zero at 12 Å. Particle-mesh Ewald summation was used for calculate the long-range electrostatic interactions. And, system was simulated under NVT conditions at 310 K temperature. This system was minimized for 10,000 steps with 2 fs time step. Then, system equilibrated for 1 ns with fixed C^{α}, after 1 ns, C^{α}s of the system was connected to the imaginary spring that has 1 $kcal/mol/Å^2$ spring constant for 2 ns. At the last system was released for 4 ns. When the system reaches the equilibrium after 7 ns equilibration simulation, lever arm of myosin VI and calmodulin was transferred larger solvation box for SMD simulation. Before transferring, IQ domain aligned to x axis. The dimensions of system was altered to 197 Å × 77 Å × 77 Å. This larger new system contains 111,369 atoms. New prepared system was equilibrated using the same procedure indicated above. Then, C^{α} of the 811^{th} residue of the lever arm of myosin VI was fixed and C^{α} of the 913^{th} residue

was selected as a SMD atom. Dummy atom was bound to the SMD atom with a virtual spring that has 5 $kcal/mol/Å^2$ constant. And, dummy atom was pulled with 2 $Å/ns$ constant velocity to direction from center of mass of the fixed atom to the center of mass of the SMD atom that was computed as 0.9906, 0.0745, and 0.1140 that are x-y-z components of the direction, respectively, for 10 ns with 1 fs time step and NVT ensemble, as described in the study [16]. Obtained system at the end of the SMD simulation, SMD and fix atoms were fixed for 10 ns for relaxing the system with 2 fs time step and NPT ensemble. Then, obtained system was followed again SMD simulations. All MD and SMD simulations were performed in NAMD 2.12 [40] with using CHARMM36 [48] force field.

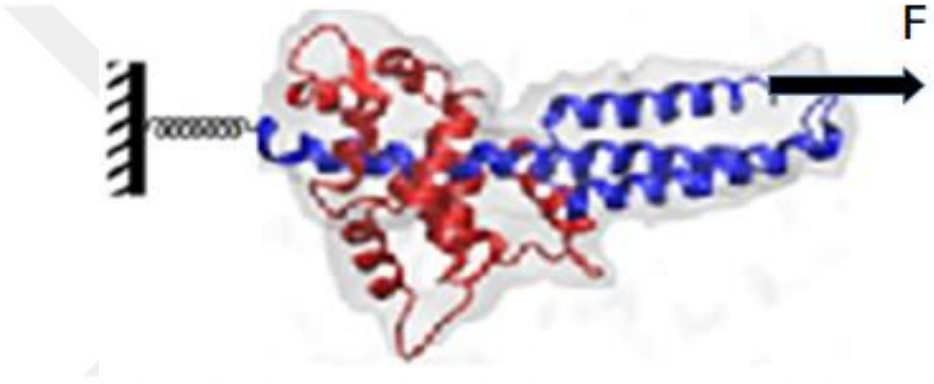

Figure 2.3: Exertion of force on residue 913.

2.4 System Preparation of Dynein Linker Movement

In this part of the study, the dynein linker movement was partially modelled. For this purpose, pre-powerstroke state conformation of linker was steered to its post-powerstroke state conformation using SMD simulations. In the literature, both pre-powerstroke and post-powerstroke structures are present (PDB 4RH7 [27] and 3VKG [26], respectively).

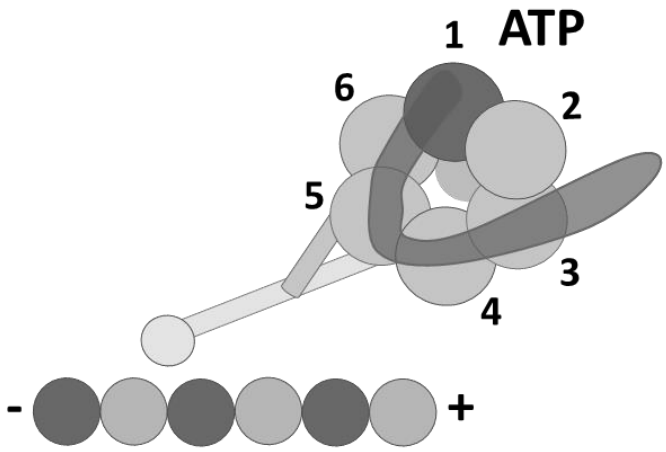

Figure 2.4: Pre-powerstroke stage structure.

Pre-powerstroke state conformation of dynein linker was used as initial structure from the recent MD data Can et al. [1]. At the beginning, 3VKG and initial structure was aligned through residues 1425-1550 of the linker as shown in Figure 2.4. Then, C^{α} atoms of residues 1264, 1309 and 1325 residues of the linker were selected as a SMD atoms. C^{α} atoms of residues 1415-1425 were fixed. Reaction coordinate of the system was selected as center of mass of the SMD atoms to corresponding atoms on the 3VKG structure. In the Figure 2.5, reaction coordinate can be seen. Dummy atom was bound to the SMD atom with a virtual spring that has 25 $kcal/mol/\text{Å}^2$ spring constant. Then, dummy atom was pulled witch 1 $\text{Å}/ns$ constant velocity for 5 ns along the steering direction followed by 10 ns of constrained MD simulation applied on SMD and fixed atoms. SMD and fixed atoms were constrained with spring that has 5 $kcal/mol/\text{Å}^2$ spring constant.

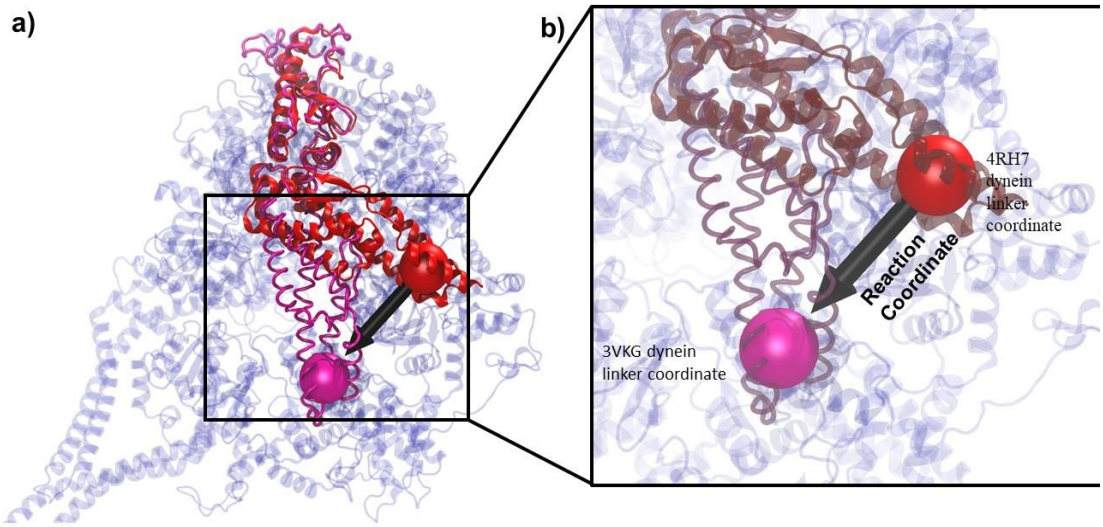

Figure 2.5: Initial structure and vector of the reaction coordinate.

2.5 Solvent Accessible Surface Area

Solvent Accessible Surface Area (SASA) is as indicated in the name surface area that accessible to solvent [49]. The accessible surface area of an atom, A, is the area of a radius R located at each point on the surface [49]. On each point, center of solvent molecule can be placed without penetrate vdW radii of the atoms. Approximation of the area is computed by;

$$accessible\ surface\ area = A = \sum(R/\sqrt{R^2 - Z_i^2}) \cdot D \cdot L_i \qquad (5)$$

$$D = \Delta Z/2\ + \Delta' Z$$

Where L_i refers length of the arc drawn on section, perpendicular distance from center of the sphere to section is referred as Z_i. Spacing between the sections is referred as ΔZ [49].

2.6 Root Mean Square Deviation

One of the distance-based measurement for protein structure similarity is Root Mean Square Deviation (RMSD) method [50]. This method gives similarity between two superimposed structure quantitatively. RMSD is calculated with this formula [50];

$$RMSD = \sqrt{\frac{1}{n}\sum_{i=1}^{n} d_i^2} \qquad (6)$$

where the n refers equivalent pair of atoms and d_i refers the distance between the i-th pair atoms [50].

2.7 Work Calculation

The conformational changes were performed by applying steering forces via a virtual spring that is connected to a dummy atom, which is pulled at a constant velocity. Since pulling takes place at a constant velocity this is a reversible process. In the constant velocity SMD simulations, λ referred as external parameter that correlated with dummy atom coordinate and changes as follows over time,

$$\lambda(t) = \lambda(0) + vt \tag{7}$$

External work of the system was evaluated as;

$$W_{\lambda(0)\rightarrow\lambda(t)} = \int_{\lambda(0)}^{\lambda(t)} F d\lambda \tag{8}$$

where F is the applied force to the system [51].

3. RESULT AND DISCUSSION

3.1 Myosin Lever Arm Structure

The first part of the thesis comprises reproducing data of the previous study by Liu et. Al [16]. and validating our results. This will allow us to conform the correct application of the methodology and apply it to a system previously not studied in the literature, which is the second part of the thesis.

3.1.1 Equilibration of myosin

As described in the methodology section, equilibration was performed for 7ns. RMSD was caluclated with respect to the crystal structure using alpha carbon atoms. The evolution of the RMSD for the proximal tail and the complete protein is shown in Figure 3.1. The first 1ns the alpha carbons of the protein were kept fixed. After that they were constrained with a force constant of 1kcal/mol Å. The RMSD immediately increased to 0.5 Å. After 3ns any constrains on the protein were removed and RMSD converged to a vlaue around 3 Å. Thus, it was concluded that structurally equilibrated myosin was obtained.

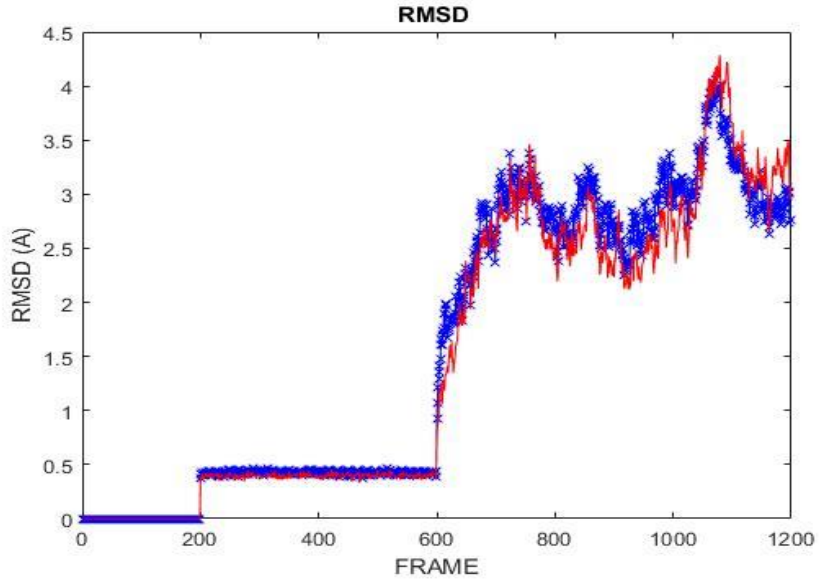

Figure 3.1: RMSD Value For all protein (blue) and proximal tail (red).

3.1.2 Steered molecular dynamics simulations of myosin proximal tail

The details of the SMD simulation protocol is described in the methodology section. Here SMD simulations followed by fixed simulations (Please refer to methodology for details) were performed. In the fixed simulations SMD atoms were fixed. This released partially the tension which build up during SMD. Thus, allowing the protein to optimize in this new proximal tail conformation. A total of 40 ns SMD and 40 ns fixed MD simulations were performed. Overally the degree of extension follows a straight line during SMD simulations. Frequently, large fluctuations are observed probably relating to bond/inetraction breakage. The characteristics of the time vs extension data we produced was in accord with the previous study in the literature by Liu et al. [16]

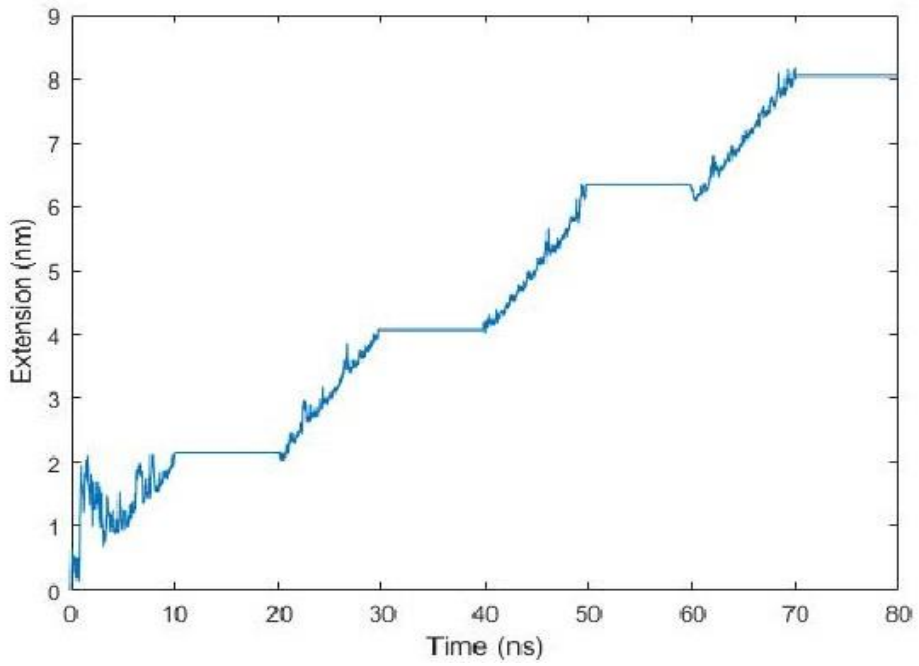

Figure 3.2: Extension of proximal tail (residue 811 to 913) of myosin VI.

3.1.3 Number of hydrogen bonds during proximal tail extension

The hydrogen-bond play a signifacant roles in proteins' structure since they stabilizes the secondary, tertiary and quaternary structure of proteins and it connects the amino acids between different polypeptide chains in proteins' structure. According to this, the number of hydrogen bonds during SMD simulations indicate the extend of which the helices in the proximal tail are broken. How hydrogen bonds were calculated during the simulations were described in the methodology section. As shown in Figure 3.3 the number of hydrogen bonds in the proximal tail decrease from 240 to 160 in total (%50). Thus, indicating a large amount of structural change.

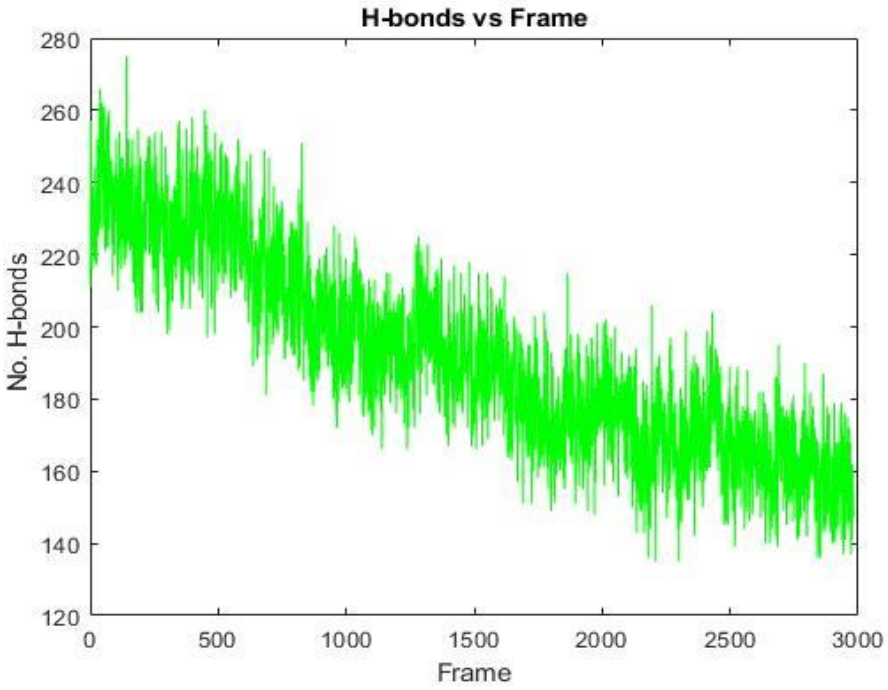

Figure 3.3: Number of hydrogen bonds during SMD.

3.1.4 Evolution of solvent accessible surface area (sasa) during proximal tail extension

Building secondary and tertiary structures generally increases the size of the protein core and the number of aminoacids in contact with the solvent. Thus investigating the change of solvent accessible surface area throughot the trajectory is an indication of the degree at which the protein bcomes unstructured. The structure which is extended via SMD simulations comprises helices and those are broken upon force application. Solvent accessible surface area was evaluated over time. As shown in Figure 3.4, there in SASA increases from approximately 49 nm^2 to 68 nm^2 (by ~40%) due to stretching the protein during 80 ns of SMD. This number is comparable in magnitude to the decrease in the number of hydrogen bonds as evaluated in the previous section.

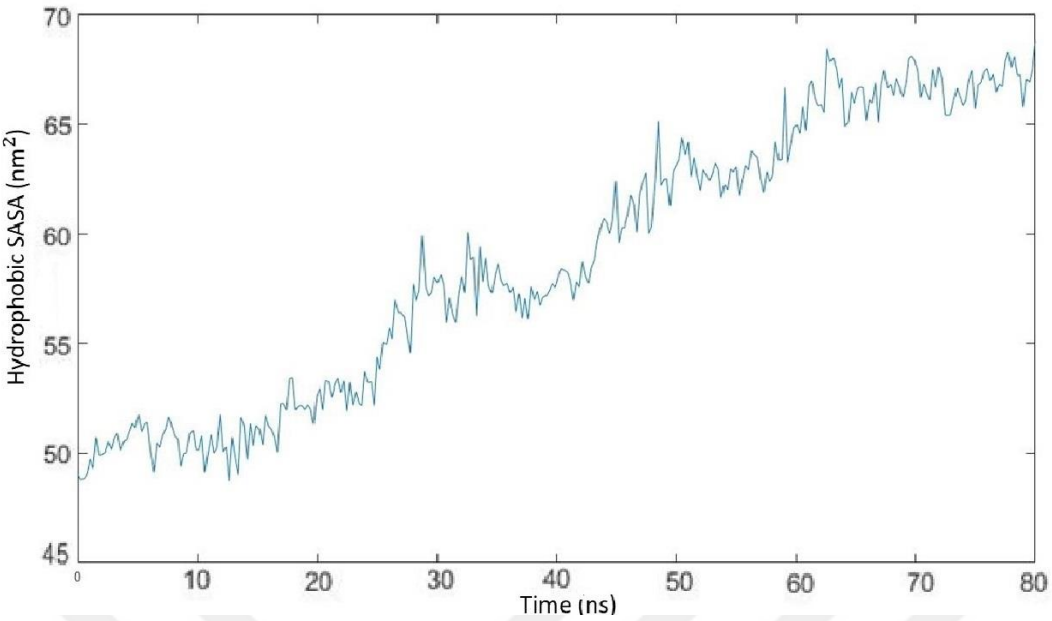

Figure 3.4: Exposed hydrophobic SASA versus time.

3.1.5 Force and work applied during proximal tail extension

As described in the methodology section, the force applied to the center of mass of the SMD atoms depends on how much this coordinate lacks behind the dummy atom coordinate. Thus using the SMD atom coordinates the force at each time instant can be evaluated via Eq.3. The force applied during the 40ns of SMD simulations is plotted in Figure 3.4. It is clearly seen that the force values are amplified in the region 1.3nm to 4.8nm. These points are highighted with arrows 2 and 3 in the figure. The force values were recorded every frame which is 25 ps and average trendline was shown in green color for visiual purposes.

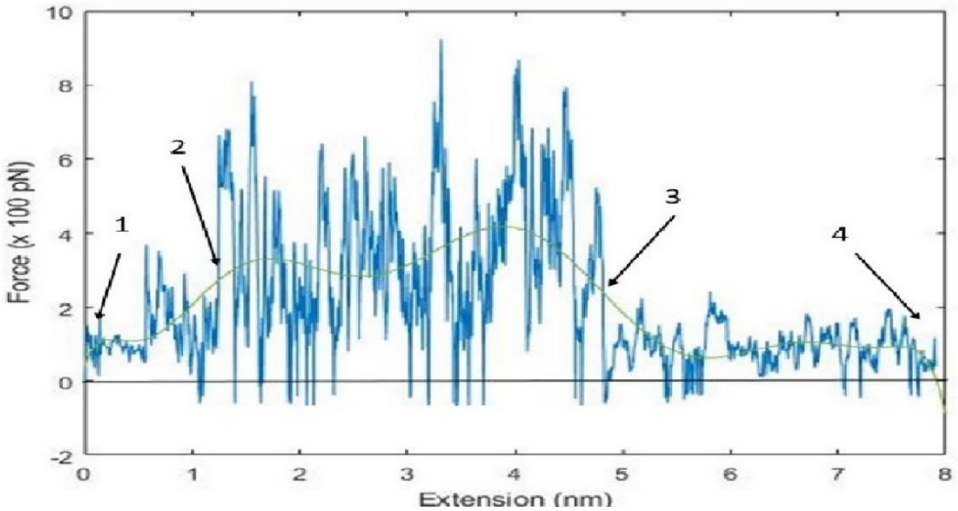

Figure 3.5: Force fluctuation versus to extension length.

In order to have a better understanding, protein conformations corresponding to time instances ar arrows 1-4 are shown in figures 3.6-3.9. As shown in the figures the largest force values are obtained alpha-helix scondary structure in the proximal tail unfolds.

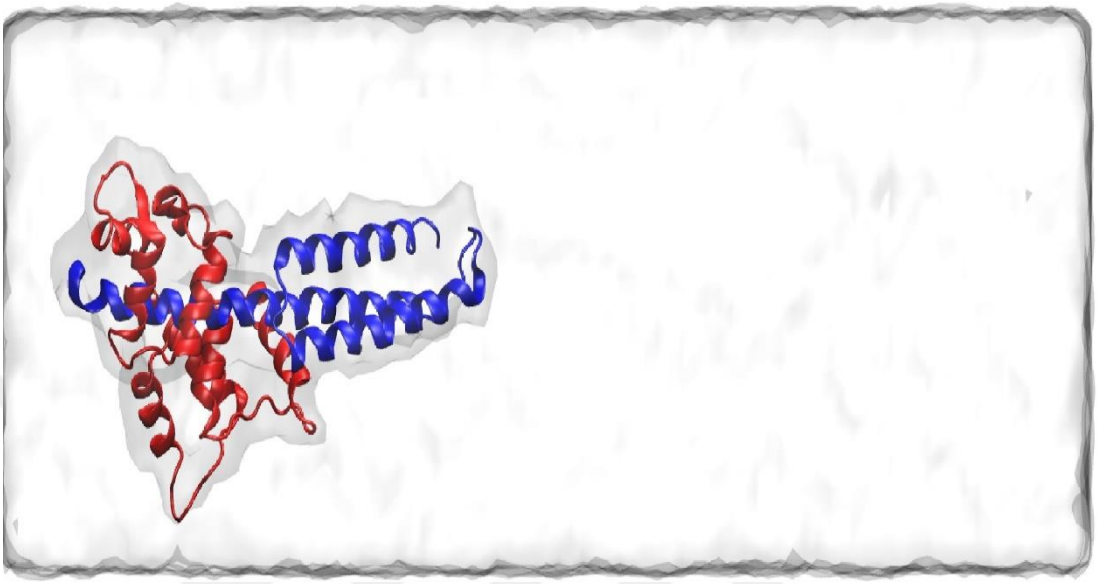

Figure 3.6: Initial coordinates of proximal tail inside the water box (point 1).

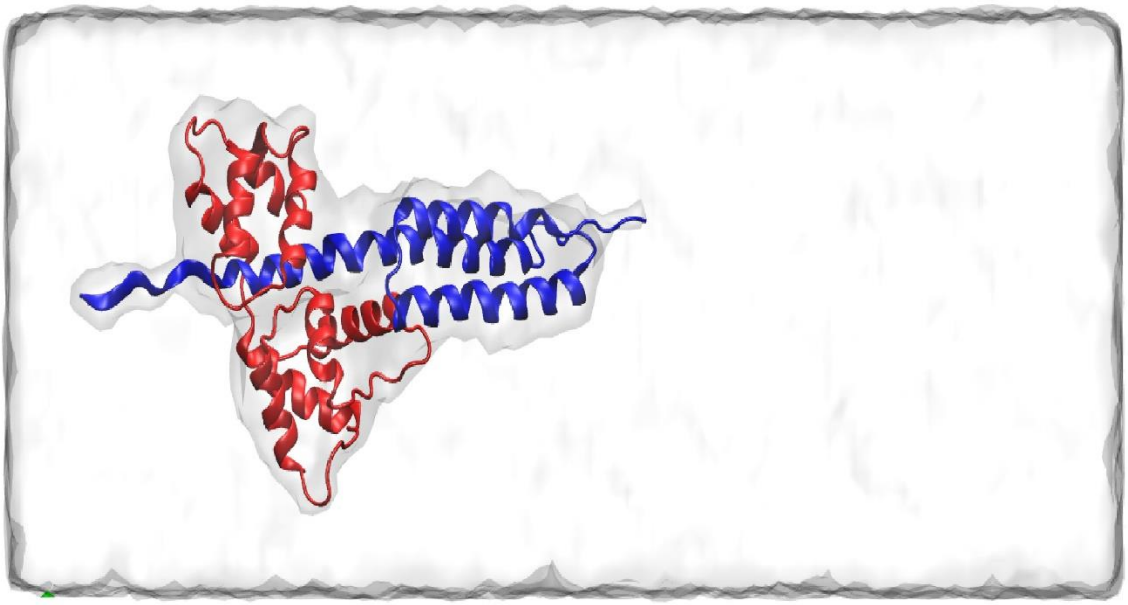

Figure 3.7: The start coordinates of unfolding alpha-helix (point 2).

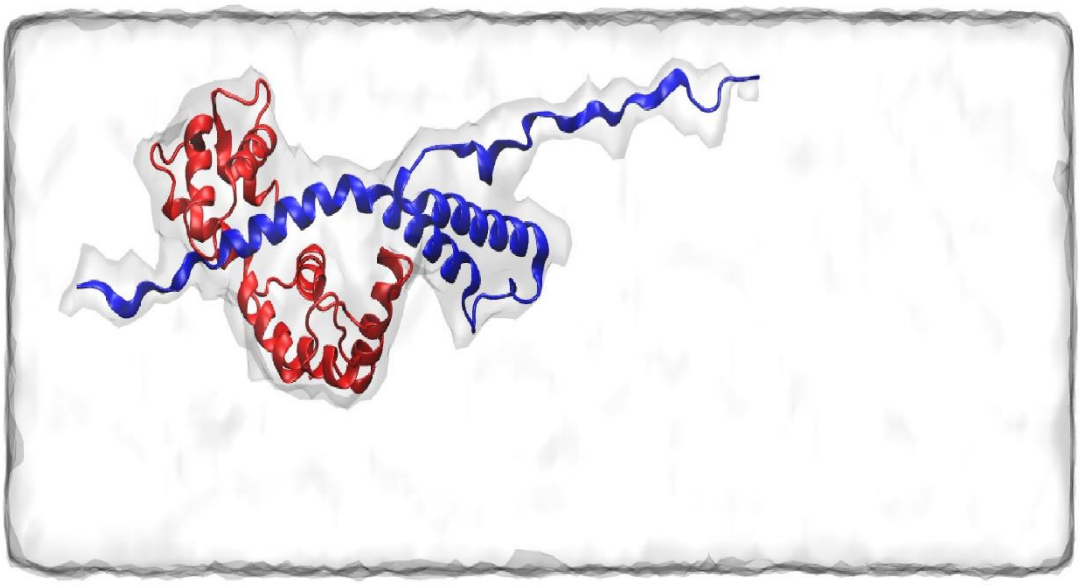

Figure 3.8: Unfolding of alpha-helix in the x-direction (point 3).

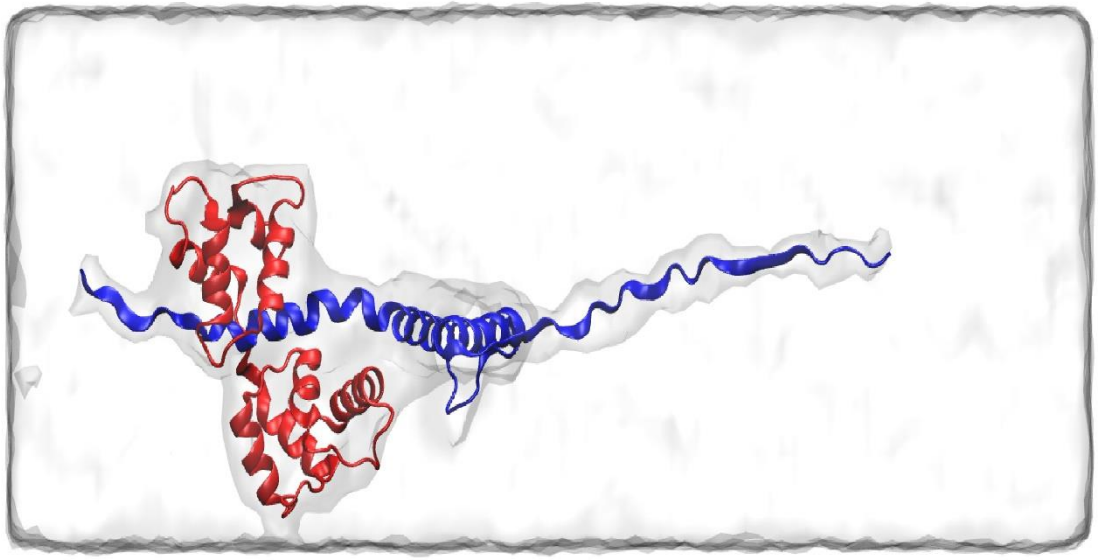

Figure 3.9: Stable structure of the proximal tail (point 4).

After third point, as expected power stroke the range of force decrease and tend to steady values which express the stabilizing of structure bypassing the energy barrier.

By using the force-extension data, the total work applied to the system can be calculated. The evolution of the total work applied over the SMD simulation length was evaluated and shown in Figure 3.10. As can be seen, the slope of the work graph is highest when the proximal tail unfolds.

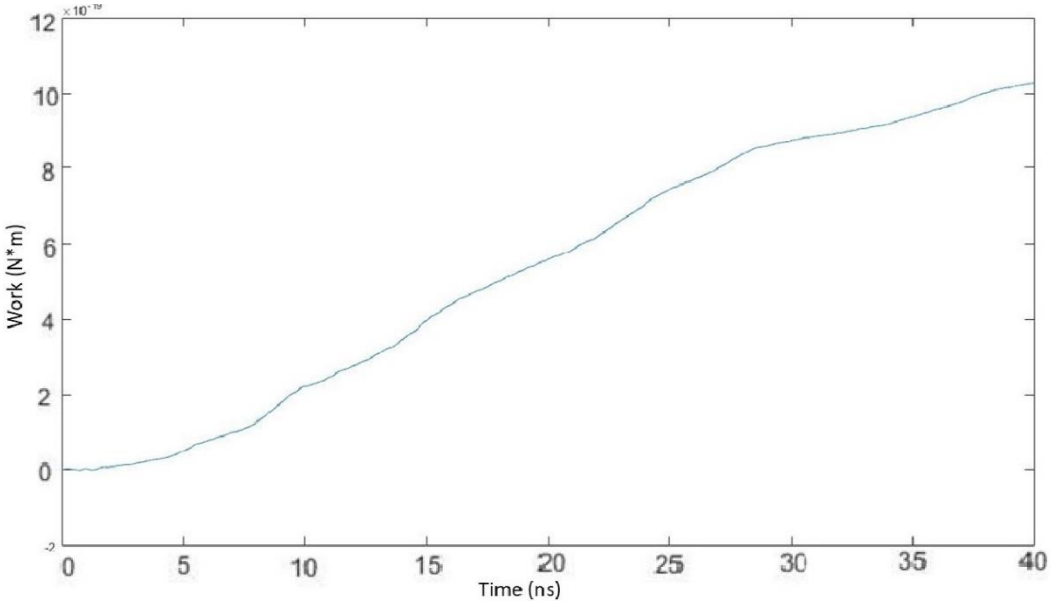

Figure 3.10: Total work during SMD simulations.

3.2 Dynein Motor Protein Linker Movement

In total 5 SMD simulations and 4 contained MD simulations were performed. Please refer to the methodology section for details. A total of 65ns of MD simulations were performed. The center of mass of the SMD atoms followed the dummy atom closely. At each constrained simulation a slight decrease in the coordinate along the pulling direction was observed; i.e. the linker tended to go backward along the steering direction.

To analyze the movement of the linker, all trajectories were aligned to initial structure through the fixed atoms and movement of the center of masses of the SMD atoms was measured through the trajectories. Dynein linker moved approximately 22 Å along the pulling direction. In the beginning, the measured distance was approximately 40 Å.

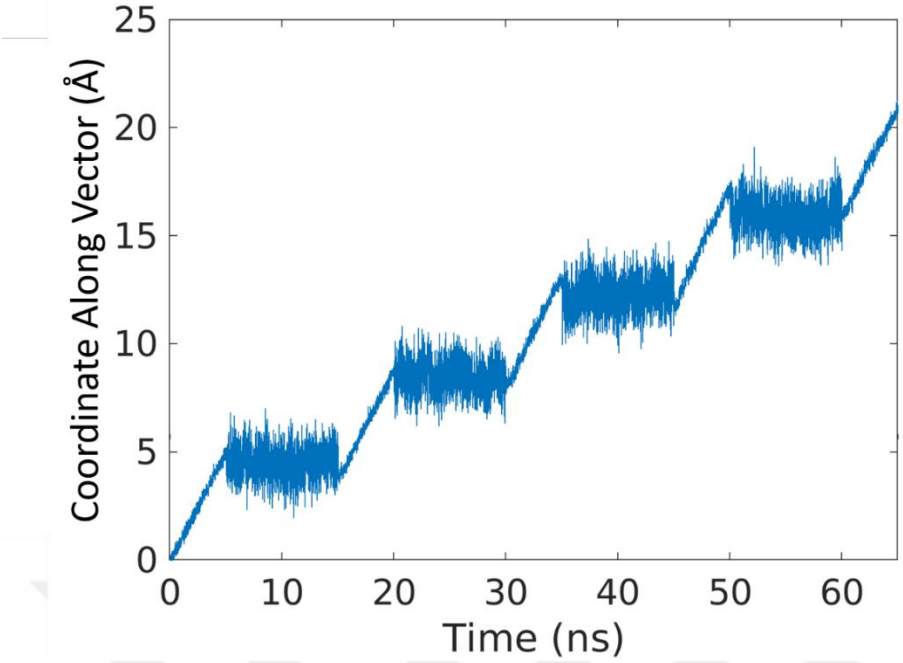

Figure 3.11: Evolution of SMD simulations along the pulling direction vector.

SMD trajectories were merged into a single trajectory and force values for each frame were evaluated. The evolution of forces along the pulling direction re shown in Figure 3.12. The work values are shown in Figure 3.13. The work graph showed the largest increase between 20 Å and 22 Å. Total work done during the simulations were calculated as 484.8 kcal/mol.

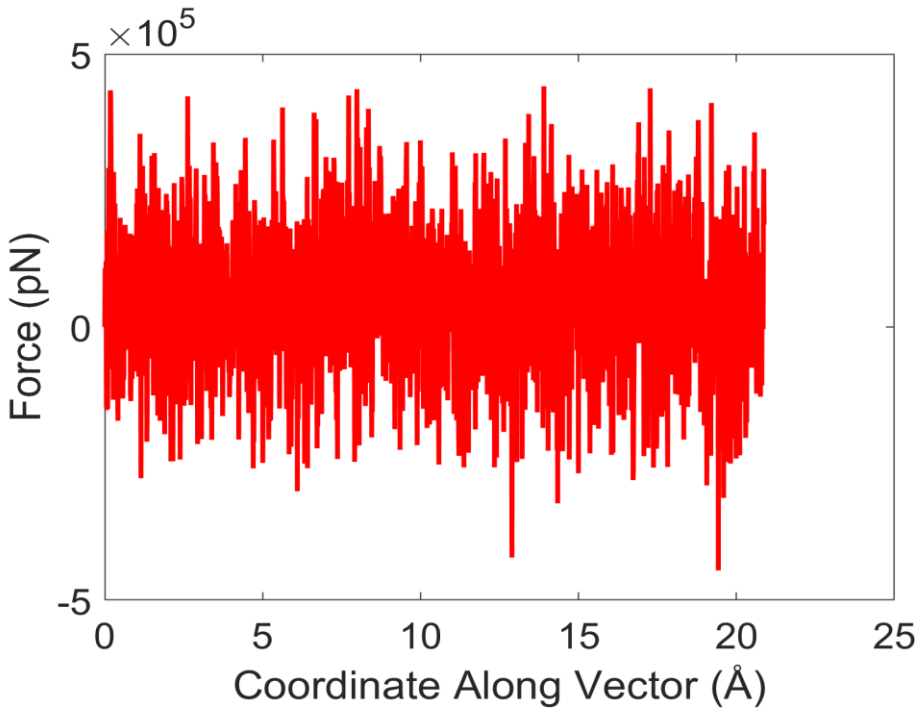

Figure 3.12: Evolution of force during SMD simulations.

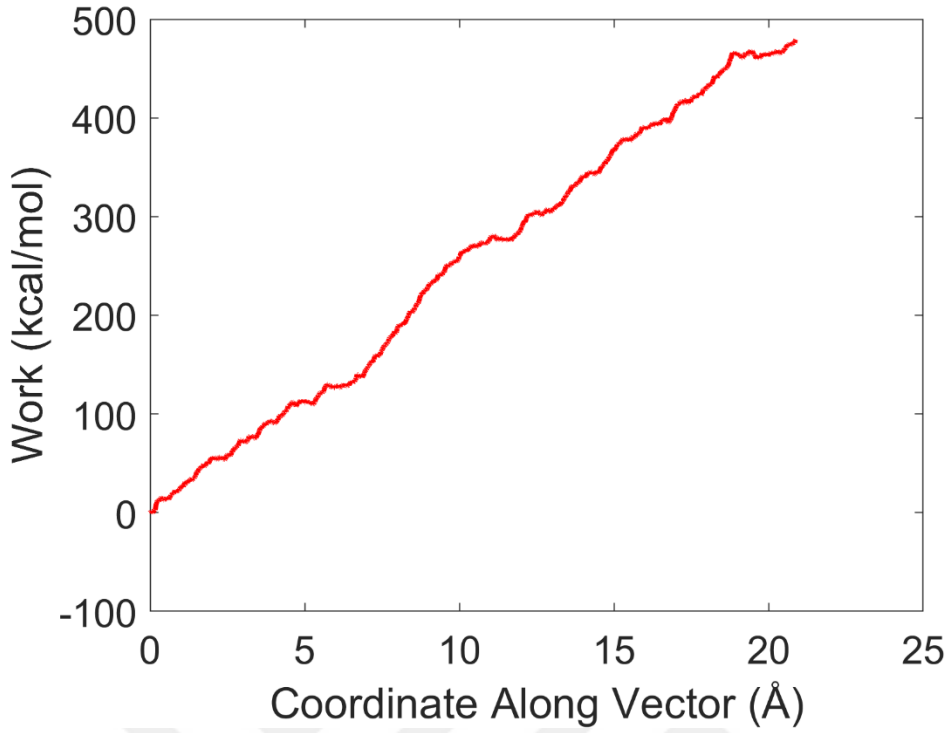

Figure 3.13: Total work during SMD simulations.

4. CONCLUSIONS AND RECOMMENDATIONS

Steered Molecular Dynamics simulations appear to be an effective Molecular Dynamics technique to model conformational changes in motor proteins. It can be applied to motor proteins in an efficient manner and results are reproducible. The reproducibility of the methodology was supported by the accord of our SMD results and thus of the earlier study by Liu et al [16]. SMD simulations applied to the linker of dynein achieved a large movement, thus, modeling a significant part of the linker conformational transition between its bent and straight conformations. However, the results clearly show that optimization in the selection of steered atoms, steered atoms, pulling vector and spring constants are required.

REFERENCES

[1] **Can, S., et al.**, Directionality of dynein is controlled by the angle and length of its stalk. Nature, 2019. 566(7744): p. 407.

[2] **Belitz, P.D.I.H.D. and P.D.I.W. Grosch**, Food Chemistry. 2013: Springer Berlin Heidelberg.

[3] **Berg JM, T.J., Stryer L**. Biochemistry. 5th edition. New York: W H Freeman; , Biochemistry. 2002.

[4] **Sweeney, H.L. and A. Houdusse**, Structural and functional insights into the myosin motor mechanism. Annual review of biophysics, 2010. 39: p. 39-557.

[5] **Spudich, J.A. and S. Sivaramakrishnan**, Myosin VI: an innovative motor that challenged the swinging lever arm hypothesis. Nature reviews Molecular cell biology, 2010. 11(2): p. 128.

[6] **Lanza, R., R. Langer, and J.P. Vacanti**, Principles of Tissue Engineering. 2013: Elsevier Science.

[7] **Cecchini, M., Y. Alexeev, and M. Karplus**, Pi release from myosin: a simulation analysis of possible pathways. Structure, 2010. 18(4): p. 458-470.

[8] **Ovchinnikov, V., B.L. Trout, and M. Karplus**, Mechanical coupling in myoyosin V: a simulation study. Journal of molecular biology, 2010. 395(4): p. 815-833.

[9] **Zheng, W.**, Multiscale modeling of structural dynamics underlying force generation and product release in actomyosin complex. Proteins: Structure, Function, and Bioinformatics, 2010. 78(3): p. 638-660.

[10] **Zheng, W. and D. Thirumalai**, Coupling between normal modes drives protein conformational dynamics: illustrations using allosteric transitions in myosin II. Biophysical journal, 2009. 96(6): p. 2128-2137.

[11] **Aschenbrenner, L., S.N. Naccache, and T. Hasson**, Uncoated endocytic vesicles require the unconventional myosin, Myo6, for rapid transport through actin barriers. Molecular biology of the cell, 2004. 15(5): p. 2253-2263.

[12] **Warner, C.L., et al.**, Loss of myosin VI reduces secretion and the size of the Golgi in fibroblasts from Snell's waltzer mice. The EMBO Journal, 2003. 22(3): p. 569-579.

[13] **Avraham, K.B., et al.**, The mouse Snell's waltzer deafness gene encodes an unconventional myosin required for structural integrity of inner ear hair cells. Nature genetics, 1995. 11(4): p. 369.

[14] **Mukherjea, M., et al.**, Myosin VI dimerization triggers an unfolding of a three-helix bundle in order to extend its reach. Molecular cell, 2009. 35(3): p. 305-315.

[15] **Yu, C., et al.**, Myosin VI undergoes cargo-mediated dimerization. Cell, 2009. 138(3): p. 537-548.

[16] **Liu, Y., et al.**, Extension of a three-helix bundle domain of myosin VI and key role of calmodulins. Biophysical journal, 2011. 100(12): p. 2964-2973.

[17] **Reck-Peterson, S.L., et al.**, The cytoplasmic dynein transport machinery and its many cargoes. Nature Reviews Molecular Cell Biology, 2018. 19(6): p. 382.

[18] **Schroer, T.A., E.R. Steuer, and M.P. Sheetz**, Cytoplasmic dynein is a minus end-directed motor for membranous organelles. Cell, 1989. 56(6): p. 937-946.

[19] **Vale, R.D.**, The Molecular Motor Toolbox for Intracellular Transport. Cell, 2003. 112(4): p. 467-480.

[20] **Burgess, S.A., et al.**, Dynein structure and power stroke. Nature, 2003. 421(6924): p. 715.

[21] **Schmidt, H., E.S. Gleave, and A.P. Carter**, Insights into dynein motor domain function from a 3.3-Å crystal structure. Nature structural & molecular biology, 2012. 19(5): p. 492.

[22] **Gibbons, I., et al.**, Multiple nucleotide-binding sites in the sequence of dynein β heavy chain. Nature, 1991. 352(6336): p. 640.

[23] **Kon, T., et al.**, Distinct functions of nucleotide-binding/hydrolysis sites in the four AAA modules of cytoplasmic dynein. Biochemistry, 2004. 43(35):. 11266-11274.

[24] **Gee, M.A., J.E. Heuser, and R.B. Vallee**, An extended microtubule-binding structure within the dynein motor domain. Nature, 1997. 390(6660): p. 636.

[25] **Carter, A.P., et al.**, Crystal structure of the dynein motor domain. Science, 2011. 331(6021): p. 1159-1165.

[26] **Kon, T., et al.**, The 2.8 Å crystal structure of the dynein motor domain. Nature, 2012. 484(7394): p. 345.

[27] **Schmidt, H., et al.**, Structure of human cytoplasmic dynein-2 primed for its power stroke. Nature, 2015. 518(7539): p. 435.

[28] **Sweeney, H.L. and A. Houdusse**, Myosin VI Rewrites the Rules for Myosin Motors. Cell, 2010. 141(4): p. 573-582.

[29] **Spink, B.J., et al.**, Long single α-helical tail domains bridge the gap between structure and function of myosin VI. Nature Structural &Amp; Molecular Biology, 2008. 15: p. 591.

[30] **Phichith, D., et al.**, Cargo binding induces dimerization of myosin VI. Proceedings of the National Academy of Sciences, 2009. 106(41): p. 17320.

[31] **Espinoza-Fonseca, L.M., D. Kast, and D.D. Thomas**, Molecular dynamics simulations reveal a disorder-to-order transition on phosphorylation of smooth muscle myosin. Biophysical journal, 2007. 93(6): p. 2083-2090.

[32] **Mugnai, M.L. and D. Thirumalai**, Kinematics of the lever arm swing in myosin VI. Proceedings of the National Academy of Sciences, 2017. 114(22): p. E4389-E4398.

[33] **Choi, J., H. Park, and C. Seok**, How does a registry change in dynein's coiled-coil stalk drive binding of dynein to microtubules? Biochemistry, 2011. 50(35): p. 7629-7636.

[34] **Redwine, W.B., et al.**, Structural basis for microtubule binding and release by dynein. Science, 2012. 337(6101): p. 1532-1536.

[35] **Nishikawa, Y., et al.**, Structure of the entire stalk region of the Dynein motor domain. Journal of molecular biology, 2014. 426(19): p. 3232-3245.

[36] **Kamiya, N., et al.**, Elastic properties of dynein motor domain obtained from all-atom molecular dynamics simulations. Protein Engineering, Design and Selection, 2016. 29(8): p. 317-325.

[37] **Can, S., et al.**, Directionality of dynein is controlled by the angle and length of its stalk. Nature, 2019. 566(7744): p. 407-410.

[38] **McCammon, J.A., B.R. Gelin, and M. Karplus**, Dynamics of folded proteins. Nature, 1977. 267(5612): p. 585-590.

[39] **Karplus, M.**, Molecular dynamics of biological macromolecules: A brief history and perspective. Biopolymers, 2003. 68(3): p. 350-358.

[40] **Phillips, J.C., et al**., Scalable molecular dynamics with NAMD. Journal of computational chemistry, 2005. 26(16): p. 1781-1802.

[41] **González, M.**, Force fields and molecular dynamics simulations. École thématique de la Société Française de la Neutronique, 2011. 12: p. 169-200.

[42] **Nosé, S.**, A molecular dynamics method for simulations in the canonical ensemble. Molecular physics, 1984. 52(2): p. 255-268.

[43] **Kadoura, A., A. Salama, and S. Sun**, Switching between the NVT and NpT ensembles using the reweighting and reconstruction scheme. Procedia Computer Science, 2015. 51: p. 1259-1268.

[44] **Izrailev, S., et al.**, Steered molecular dynamics, in Computational molecular dynamics: challenges, methods, ideas. 1999, Springer. p. 39-65.

[45] **Isralewitz, B., M. Gao, and K. Schulten**, Steered molecular dynamics and mechanical functions of proteins. Current opinion in structural biology, 2001. 11(2): p. 224-230.

[46] **Kalé, L., et al.**, NAMD2: Greater Scalability for Parallel Molecular Dynamics. Journal of Computational Physics, 1999. 151(1): p. 283-312.

[47] **Humphrey, W., A. Dalke, and K. Schulten**, VMD: visual molecular dynamics. Journal of molecular graphics, 1996. 14(1): p. 33-38.

[48] **Best, R.B., et al.**, Optimization of the additive CHARMM all-atom protein force field targeting improved sampling of the backbone ϕ, ψ and side-chain χ1 and χ2 dihedral angles. Journal of chemical theory and computation, 2012. 8(9): p. 3257-3273.

[49] **Lee, B. and F.M. Richards**, The interpretation of protein structures: estimation of static accessibility. Journal of molecular biology, 1971. 55(3): p. 379-IN4.

[50] **Kufareva, I. and R. Abagyan**, Methods of protein structure comparison, in Homology Modeling. 2011, Springer. p. 231-257.

CURRICULUM VITAE

Name Surname : **Mohammad Amin SALEHI TABRIZI**

Place and Date of Birth : **Tabriz / 13.09.1988**

E-Mail : **tabrizi15@itu.edu.tr**

Amin.spinas@gmail.com

EDUCATION

- **B.Sc.** : University of Tabriz, Mechanical Eng. Dept (Iran)
- **M.Sc.** : Istanbul Technical University, Mechanical Engineering Department (Turkey)